

Extension of the Alkane Bridge in BisNHC–Palladium–Chloride Complexes. Synthesis, Structure, and Catalytic Activity

Sebastian Ahrens, Alexander Zeller, Maria Taige, and Thomas Strassner*

Physikalische Organische Chemie, Technische Universität Dresden,
Mommssenstrasse 13, D-01062 Dresden, Germany

Received June 29, 2006

A series of bisNHC chelate ligands with alkyl bridges of different chain lengths and their palladium complexes have been prepared. The influence of the different bridges on the solid-state structure and reactivity of the complexes has been studied. The catalytic activity of the palladium complexes was successfully tested in the Mizoroki–Heck reaction and the catalytic CH activation of methane. The ethylene-bridged palladium complex showed the highest catalytic activity in the CH activation of methane and the Mizoroki–Heck coupling of bromoarenes, while for unreactive chloroarenes bisNHC complexes with longer bridges give better results.

1. Introduction

N-Heterocyclic carbenes (NHCs) are often considered as alternatives for phosphine ligands in homogeneous catalysis.^{1,2} There are many examples of monodentate NHCs, but only a few examples of alkane-bridged chelating biscarbene ligands. Chelated carbenes are expected to be more stable since one possible decomposition pathway, reductive elimination of the carbene, should be slower for this conformationally restricted case. A chelating coordination is one way to obtain highly stable catalysts capable of tolerating harsher reaction conditions than traditional phosphine catalysts. Others^{3–12} and we^{13–15} have published chelating palladium and platinum biscarbene compounds, but considering alkyl chains until now only methylene- and ethylene-bridged compounds for palladium and platinum

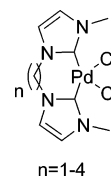


Figure 1. Palladium biscarbene chloride complexes with different alkyl bridge lengths.

were known.^{11,13,16–18} Very recent publications reported the first examples of iridium, ruthenium, and rhodium complexes^{19–21} with longer alkane-bridged biscarbene ligands. Here we describe a novel synthetic pathway leading to palladium bisNHC–bischloride complexes with different alkyl bridge lengths (Figure 1).

These bidentate chelating carbenes provide an excellent way to study the effects of ligand anisotropy on the reactivity of the complexes formed.²⁰ The palladium complexes have also been tested in the catalytic CH activation of methane and the Heck reaction of chloro- and bromoarenes.

Methane as the cheapest of all hydrocarbons is readily available from natural gas feedstock and has been utilized as a raw material for the production of energy and other products such as hydrogen for many decades. Nevertheless, an efficient, direct functionalization of methane under mild conditions remains a difficult challenge to chemists even today. If successful, such new processes may give rise to cleaner and more efficient alternatives to existing technology.²²

Palladium complexes have also been widely used as catalysts for carbon–carbon bond forming reactions. These reactions are key steps in many syntheses as well as in a variety of industrial

* Corresponding author. Tel: +49(0)351-463 38571 Fax: +49(0)351-463 39679. E-mail: thomas.strassner@chemie.tu-dresden.de.

(1) Arduengo, A. J., III; Dias, H. V. R.; Harlow, R. L.; Kline, M. *J. Am. Chem. Soc.* **1992**, *114* (14), 5530–5534.

(2) Herrmann, W. A. *Angew. Chem., Int. Ed.* **2002**, *41* (8), 1290–1309.

(3) Heckenroth, M.; Neels, A.; Stoeckli-Evans, H.; Albrecht, M. *Inorg. Chim. Acta* **2006**, *359* (6), 1929–1938.

(4) Öfele, K.; Herrmann, W. A.; Mihalios, D.; Elison, M.; Herdtweck, E.; Priemeier, T.; Kiprof, P. *J. Organomet. Chem.* **1995**, *498* (1), 1–14.

(5) Kernbach, U.; Ramm, M.; Luger, P.; Fehlhammer, W. P. *Angew. Chem., Int. Ed. Engl.* **1996**, *35* (3), 310–312.

(6) Frankel, R.; Kernbach, U.; Bakola-Christianopoulou, M.; Plaia, U.; Suter, M.; Ponikvar, W.; Noth, H.; Moinet, C.; Fehlhammer, W. P. *J. Organomet. Chem.* **2001**, *617–618*, 530–545.

(7) Danopoulos, A. A.; Tulloch, A. A. D.; Winston, S.; Eastham, G.; Hursthouse, M. B. *Dalton Trans.* **2003** (5), 1009–1015.

(8) Miecznikowski, J. R.; Gruendemann, S.; Albrecht, M.; Megret, C.; Clot, E.; Faller, J. W.; Eisenstein, O.; Crabtree, R. H. *Dalton Trans.* **2003** (5), 831–838.

(9) Gruendemann, S.; Albrecht, M.; Kovacevic, A.; Faller, J. W.; Crabtree, R. H. *Dalton Trans.* **2002** (10), 2163–2167.

(10) Peris, E.; Mata, J.; Loch, J. A.; Crabtree, R. H. *Chem. Commun.* **2001** (2), 201–202.

(11) Quezada, C. A.; Garrison, J. C.; Tessier, C. A.; Youngs, W. J. *J. Organomet. Chem.* **2003**, *671* (1–2), 183–186.

(12) Crabtree, R. H. *J. Organomet. Chem.* **2005**, *690* (24–25), 5451–5457.

(13) Muehlhofer, M.; Strassner, T.; Herdtweck, E.; Herrmann, W. A. *J. Organomet. Chem.* **2002**, *660* (2), 121–126.

(14) Strassner, T.; Muehlhofer, M.; Zeller, A.; Herdtweck, E.; Herrmann, W. A. *J. Organomet. Chem.* **2004**, *689* (8), 1418–1424.

(15) Ahrens, S.; Herdtweck, E.; Goutal, S.; Strassner, T. *Eur. J. Inorg. Chem.* **2006**, *2006* (6), 1268–1274.

(16) Jin, C.-M.; Twamley, B.; Shreeve, J. M. *Organometallics* **2005**, *24* (12), 3020–3023.

(17) Lee, H. M.; Lu, C. Y.; Chen, C. Y.; Chen, W. L.; Lin, H. C.; Chiu, P. L.; Cheng, P. Y. *Tetrahedron* **2004**, *60* (27), 5807–5825.

(18) Douthwaite, R. E.; Green, M. L. H.; Silcock, P. J.; Gomes, P. T. *Dalton Trans.* **2002** (7), 1386–1390.

(19) Poyatos, M.; Mas-Marza, E.; Sanau, M.; Peris, E. *Inorg. Chem.* **2004**, *43* (5), 1793–1798.

(20) Viciano, M.; Poyatos, M.; Sanau, M.; Peris, E.; Rossin, A.; Ujaque, G.; Lledos, A. *Organometallics* **2006**, *25* (5), 1120–1134.

(21) Viciano, M.; Mas-Marza, E.; Sanau, M.; Peris, E. *Organometallics* **2006**, *25* (12), 3063–3069.

(22) Lersch, M.; Tilset, M. *Chem. Rev.* **2005**, *105* (6), 2471–526.

Scheme 1. Synthesis of Alkyl-Bridged Bisimidazoliumchlorides

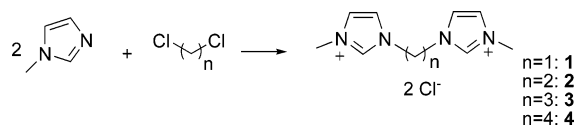


Table 1. Yields of Alkyl-Bridged Bisimidazolium Chlorides

	1	2	3	4
yield (%)	64.7	78.2	76.5	55.3

processes.²³ Since its discovery in 1971,^{24,25} the Mizoroki–Heck reaction has developed into a standard method for C–C coupling, especially for iodo- or bromoarenes.²⁶ However, even today only a few catalysts are known to undergo this reaction with inexpensive chloroarenes.^{27–33}

2. Results and Discussion

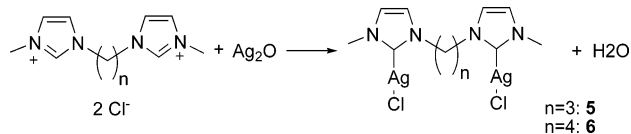
2.1. Preparation of Alkyl-Bridged Bisimidazolium Salts.

The different bisimidazolium salts can be prepared in only one step by a substitution reaction of 1-methylimidazole with different dichloroalkanes according to Scheme 1.

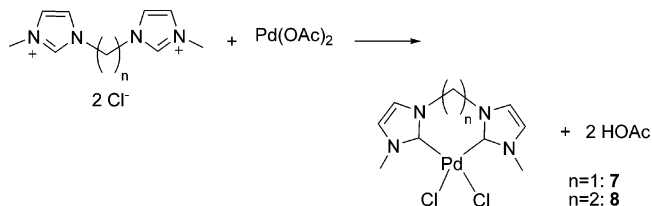
Until now the direct one-pot–one-step substitution reaction has not been possible using dichloromethane. Heinekey et al. synthesized this imidazolium salt with chloride anions by first bridging 1-methylimidazole with diiodomethane followed by six anion exchange steps,³⁴ while the corresponding palladium complex was first published by us, involving an anion exchange procedure in the metal complex preparation step.¹⁴ However if the direct substitution reaction is carried out in poly(ethylene glycol) 200 (PEG 200), the desired product is obtained in only one step in good yield and purity.³⁵ While the reaction of 1-methylimidazole with dichloromethane is possible only in PEG, the other reactions can also be accomplished neat or in THF. Yields of the bisimidazolium chloride salts are given in Table 1.

2.2. Preparation of the Silver Complexes. The synthesis of the palladium(II) complexes with methylene and ethylene bridges (**7**, **8**) is possible via direct deprotonation of the imidazolium salts with the basic metal precursor palladium acetate. However, for longer alkyl bridges ($n = 3, 4$) this reaction leads to unwanted side reactions, forming complex

Scheme 2. Synthesis of Silver Complexes



Scheme 3. Synthesis of Methylene- and Ethylene-Bridged Palladium(II) NHC Complexes



mixtures of different compounds, which are difficult to separate. Milder reaction conditions and lower temperatures are needed; therefore we first synthesized the corresponding silver carbene complexes (Scheme 2), followed by transmetalation of the silver carbene complex with cycloocta-1,5-dienepalladium(II) chloride.

In contrast to the common procedure, the preparation of the silver complex was carried out in acetonitrile instead of dichloromethane.³⁶ The advantage is that the reactants completely dissolve in acetonitrile, while the desired product precipitates during the reaction. Thus, the reaction progress can be easily monitored and the analytically pure product can be isolated simply by filtration.

2.3. Preparation and Solid-State Structures of the Palladium Complexes. The palladium complexes with short alkyl bridges ($n = 1, 2$) can be obtained by direct reaction of the imidazolium salt with palladium acetate in hot DMSO according to Scheme 3. While for the methylene-bridged palladium complexes this has already been published by our group for the analogous complexes bearing bromide and iodide counterions,^{37,38} now also the chloride complex is directly accessible. In contrast to earlier findings of Lee et al.,¹⁷ the preparation of **8** was successful using a slightly modified temperature program for the synthesis.

Single crystals for the solid-state structure determinations of **7** and **8** could be obtained by slowly cooling of a hot saturated DMSO solution. The solid-state structure of **7** is shown in Figure 2, and the solid-state structure of **8** in Figure 4.

One solvent molecule (DMSO) is found in the unit cell of the solid-state structure of **7**, which forms a weak CH–O interaction between the oxygen atom of the DMSO molecule and one of the acidic protons of the methylene bridge (C5) between the two NHCs. The distance between H5B and O1 is found to be only 2.135 Å. There are also two other short contacts between the chloride ions of the complex and one of the hydrogens of each methyl group of the DMSO molecule. The distance between Cl1 and H20C is found to be 2.942 Å; the distance between Cl2 and H19B, 2.904 Å. These short contacts are shown in Figure 3. According to DFT calculations, these interactions are stabilized by a free energy difference of $\Delta G = -4.7$ kcal/mol. Computational details are given in the Experimental Section.

In the solid-state structure of **8** (Figure 4) the ethylene bridge is slightly twisted to accommodate the bigger ring size. This

(23) Cornils, B.; Herrmann, W. A. *Applied Homogeneous Catalysis with Organometallic Compounds*, 2nd ed.; VCH: Weinheim, 2002.

(24) Mizoroki, T.; Mori, K.; Ozaki, A. *Bull. Chem. Soc. Jpn.* **1971**, *44* (2), 581.

(25) Heck, R. F.; Nolley, J. P., Jr. *J. Org. Chem.* **1972**, *37* (14), 2320–2322.

(26) Heck, R. F. *Palladium Reagents in Organic Syntheses*; Academic Press: London, UK, 1985; p 276–287.

(27) Bohm, V. P. W.; Herrmann, W. A. *Chem. Eur. J.* **2000**, *6* (6), 1017–1025.

(28) Herrmann, W. A.; Brossmer, C.; Oefele, K.; Reisinger, C.-P.; Priermeier, T.; Beller, M.; Fischer, H. *Angew. Chem., Int. Ed. Engl.* **1995**, *34* (17), 1844–1847.

(29) Riermeier, T. H.; Zapf, A.; Beller, M. *Top. Catal.* **1998**, *4* (3, 4), 301–309.

(30) Ehrentraut, A.; Zapf, A.; Beller, M. *Synlett* **2000** (11), 1589–1592.

(31) Littke, A. F.; Fu, G. C. *J. Am. Chem. Soc.* **2001**, *123* (29), 6989–7000.

(32) Schnyder, A.; Aemmer, T.; Indolese, A. F.; Pittelkow, U.; Studer, M. *Adv. Synth. Catal.* **2002**, *344* (5), 495–498.

(33) Selvakumar, K.; Zapf, A.; Beller, M. *Org. Lett.* **2002**, *4* (18), 3031–3033.

(34) Vogt, M.; Pons, V.; Heinekey, D. M. *Organometallics* **2005**, *24* (8), 1832–1836.

(35) Strassner, T.; Ahrens, S.; Zeller, A. WO 2006058535 A2, 2006.

(36) Wang, H. M. J.; Lin, I. J. B. *Organometallics* **1998**, *17* (5), 972–975.

(37) Muehlhofer, M.; Strassner, T.; Herrmann, W. A. *Angew. Chem., Int. Ed.* **2002**, *41* (10), 1745–1747.

(38) Herdtweck, E.; Muehlhofer, M.; Strassner, T. *Acta Crystallogr., Sect. E* **2003**, *E59* (11), m970–m971.

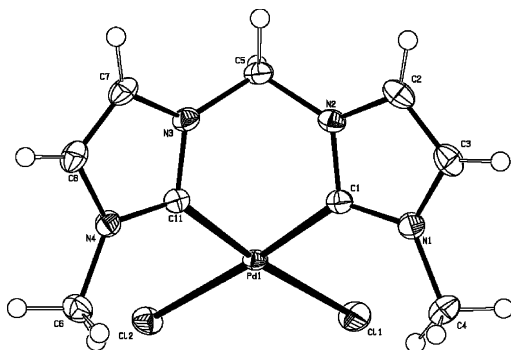


Figure 2. Solid-state structure of **7** (DMSO omitted for clarity). Ellipsoids are given at the 50% probability level.

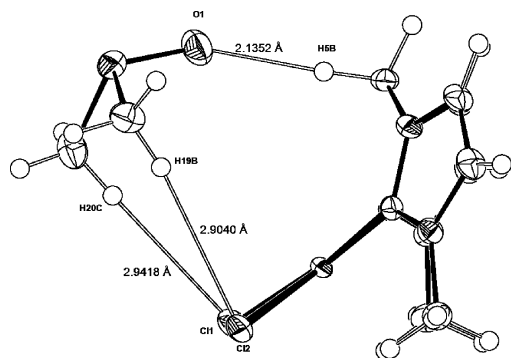


Figure 3. Short contacts between **7** and DMSO.

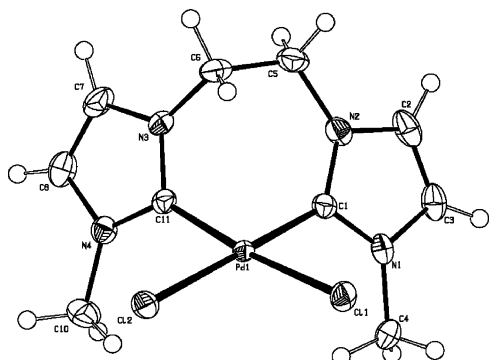


Figure 4. Solid-state structure of **8**. Ellipsoids are given at the 50% probability level.

twisted bridge is also observed in the solid-state structure of **10** and can be explained with the preferred *trans*-arrangement of the chain, which is easier to accommodate with an even number of carbon atoms between the imidazoles.

We did not succeed with the direct deprotonation in the case of imidazolium salts with alkyl bridges longer than two carbon atoms with palladium(II) acetate; we had to add an additional transmetalation step. Silver oxide was used to deprotonate the imidazolium salts. Transmetalation was then carried out using (COD)PdCl₂; both steps are done at room temperature to avoid unwanted side reactions.

The solid-state structures of the palladium complexes **9** and **10** could also be determined (Figures 5 and 6). In contrast to the solid-state structure of **7**, the planes of the imidazole rings here are less V-shaped than in the ligand, which contains a methylene bridge. While in the solid-state structure of **7** the distances N1–N4 (4.8999(18) Å) and N2–N3 (2.3547(18) Å) of the imidazole rings are quite different, the differences become smaller with increasing bridge length (**8**: 4.752(4) Å, 3.045(4) Å; **9**: 4.223(4) Å, 3.506(4) Å; **10**: 4.175(3) Å, 3.963(3) Å).

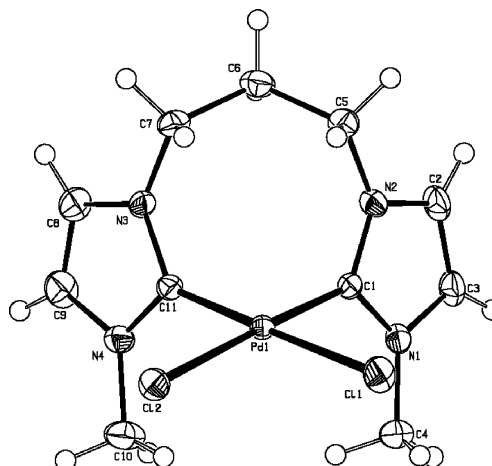


Figure 5. Solid-state structure of **9**. Ellipsoids are given at the 50% probability level.

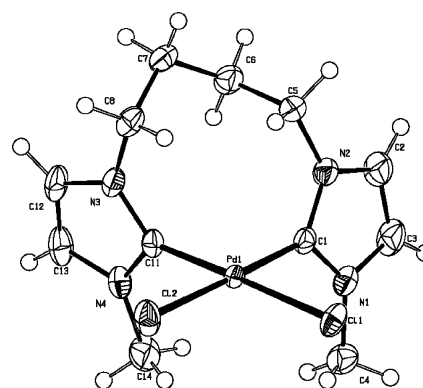


Figure 6. Solid-state structure of **10** (disordered DMSO molecule omitted for clarity). Ellipsoids are given at the 50% probability level.

Table 2. Important Geometrical Parameters^a of the Solid-State Structures of **7, **8**, **9**, and **10****

	7	8	9	10
Pd(1)–C(1)	1.9660(14)	1.979(3)	1.969(3)	1.976(2)
Pd(1)–C(11)	1.9753(14)	1.958(3)	1.973(3)	1.978(2)
Pd(1)–Cl(1)	2.3649(4)	2.3642(8)	2.3547(8)	2.3705(7)
Pd(1)–Cl(2)	2.3645(4)	2.3551(8)	2.3615(8)	2.3639(7)
C(1)–Pd(1)–C(11)	83.78(6)	87.84(11)	87.63(12)	91.15(9)
C(1)–Pd(1)–Cl(1)	92.85(4)	89.94(8)	88.76(8)	88.07(7)
Cl(1)–Pd(1)–Cl(2)	90.327(15)	91.40(2)	92.68(3)	93.66(2)
N(1)–C(1)–Pd(1)–Cl(1)	49.47(15)	57.9(3)	74.1(3)	70.3(2)

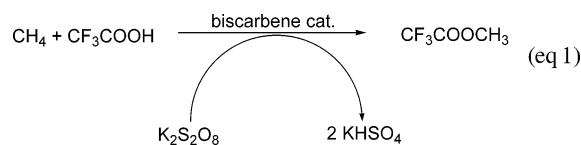
^a Distances in angstroms and angles in degrees.

With respect to important bond lengths and angles several trends are observed. The palladium carbon bond lengths are equivalent within the margin of error. The same applies for the palladium chloride bonds. The biggest differences are found in the bond angles around the metal. The C–Pd–C angle increases with the length of the bridge from 83.78(6)° in complex **7** to 87.84(11)° and 87.63(12)° in complexes **8** and **9** to 91.15(9)° in complex **10**, indicating a greater steric demand of the ligands. The growing steric demand of the ligand is also supported by the distance of the methyl groups, which shield the metal from the lower side of the complex. This distance becomes smaller with growing bridge length (**7**: 3.559, 3.548 Å; **8**: 3.337, 3.539 Å; **9**: 3.385, 3.347 Å; **10**: 3.346, 3.402 Å). Complex **10** is, to the best of our knowledge, the only *cis*-coordinated example of a C–Pd–C angle in bridged palladium(II) biscarbene complexes greater than 90°. As a result of the strong *trans* effect

of the carbene, the Cl–Pd–Cl angle also increases with growing bridge length from 90.327(15)° in complex **7**, to 91.40(2)° in **8**, to 92.68(3)° in complex **9**, and to 93.66(2)° in complex **10**, while the corresponding C–Pd–Cl angles decrease. Details of the structure determinations are given in the Experimental Section. Important geometrical parameters are given in Table 2.

3. Catalysis

3.1. Direct CH Activation of Methane. An efficient, direct functionalization of methane under mild conditions remains a difficult challenge to chemists even today. The main problem in the direct functionalization of methane is that only the first bond and not the second or more bonds must be modified. In the direct oxidation of methane to methanol, the CH bonds of methanol are less stable than in methane. The problem is overcome by intercepting methanol in the form of a methyl ester by choosing strong acids as reaction media. Equation 1 shows the oxidative character of the reaction which formally can be described as $\text{CH}_4 \rightarrow [\text{CH}_3]^+ + \text{H}^+ + 2\text{e}^-$.³⁷



The activity of complexes **7–10** in the catalytic conversion of methane to the trifluoroacetic acid methyl ester was tested in order to elucidate the influence of the ligand on the CH activation of methane. The reactions were conducted in a 160 mL Hastelloy C-2000 autoclave (Parr) in the presence of catalytic amounts of a palladium catalyst and $\text{K}_2\text{S}_2\text{O}_8$ (100 equiv) in a mixture of trifluoroacetic acid and its anhydride. The reaction vessel is pressurized with 30 bar of methane and then heated to 90 °C. These reaction conditions are the same as in previous experiments,¹⁴ except that a smaller reaction vessel of 160 mL instead of 200 mL is used. Details of the experimental setup are given in the Experimental Section; the results are given in Table 3.

The most active catalyst for the CH activation of methane and its oxidation to the trifluoroacetic acid methyl ester is found to be complex **8**. The catalytic activity of complex **8** for the CH activation of methane is the best found so far for palladium biscarbene complexes.^{14,37} The methylene-bridged palladium complex **7** and also the tetramethylene-bridged complex **10** are also quite active in the CH activation of methane, while the reactivity of complex **9** is significantly lower.

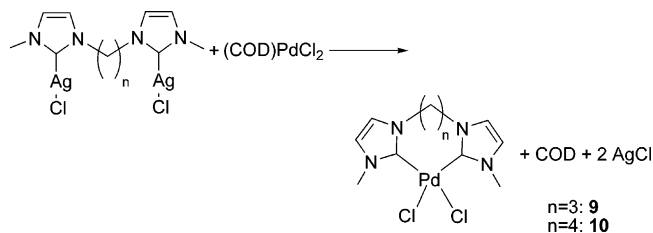
3.2. Catalytic Heck Reaction. Parallel to the catalytic CH activation of methane we also tested the catalysts in the Mizoroki–Heck reaction (Scheme 5). The results are given in Table 4.

The results show that catalyst **8** performs best in the coupling of bromoarenes. Even with concentrations of only 0.001 mol % catalyst, full conversion of the reactants is reached within 30 h. There is a high selectivity for the *trans* product in this reaction for all complexes tested. Only small amounts of the

Table 3. Results of the Catalytic CH Activation of Methane

entry	catalyst	mmol catalyst	mmol % catalyst	<i>t</i> [h]	conversion [%]	TON
1	7	0.168	0.133	17	3.2	24.0
2	8	0.168	0.133	17	4.5	33.0
3	9	0.168	0.133	17	2.4	16.8
4	10	0.168	0.133	17	3.3	25.0

Scheme 4. Synthesis of Palladium(II) NHC Complexes with Longer Alkyl Bridges



Scheme 5. Conditions of the Mizoroki–Heck Reaction

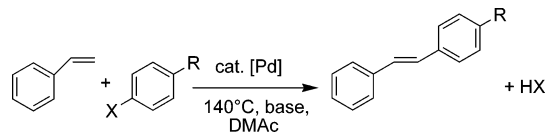


Table 4. Results of the Mizoroki–Heck Reaction

entry	R	X	cat.	mol % catalyst	<i>t</i> [h]	conversion [%]	TON	TOF [h ⁻¹]
1	C(O)CH ₃	Br	7	0.01	8.0	64 (2% <i>cis</i>)	4571	571
2	C(O)CH ₃	Br	8	0.01	7.3	100 (2% <i>cis</i>)	7143	978
3	C(O)CH ₃	Br	9	0.01	7.3	100 (1% <i>cis</i>)	7143	978
4	C(O)CH ₃	Br	10	0.01	7.3	100 (3% <i>cis</i>)	7143	978
5	C(O)CH ₃	Br	8	0.001	30.0	99 (3% <i>cis</i>)	70 714	2357
6	C(O)CH ₃	Br	9	0.001	30.0	84 (3% <i>cis</i>)	60 000	2000
7	C(O)CH ₃	Br	10	0.001	30.0	88 (1% <i>cis</i>)	62 857	2095
8	C(O)CH ₃	Cl	7	0.5	30.0	0.7	1	0
9	C(O)CH ₃	Cl	8	0.5	30.0	0	0	0
10	C(O)CH ₃	Cl	9	0.5	30.0	0.3	0.4	0
11	C(O)CH ₃	Cl	10	0.5	30.0	10	14	0

corresponding *cis* product could be detected after the reaction. Although we used higher concentrations of the catalysts for chloroacetophenone, the results are not impressive. For the less reactive chloroarenes only the tetramethylene-bridged complex **10** reaches a conversion of up to 10% within 30 h.

4. Conclusion

In this work we present the syntheses, solid-state structures, and reactivity studies of chelated biscarbene palladium(II) complexes with alkyl bridges of different lengths. The complexes are tested in the catalytic CH activation of methane and the Mizoroki–Heck reaction. Especially the ethylene-bridged complex **8** shows good activity in the CH activation of methane and in the CC coupling of bromoarenes with styrene. Here full conversion is reached with only 0.001 mol % of the catalyst. Unfortunately, complex **8** is not active at all in the coupling reaction of chloroarenes with styrene, but with the tetramethylene-bridged complex **10** it is also possible to functionalize the unreactive chloroarenes, although for good yields higher catalyst concentrations are needed.

5. Experimental Section

5.1. General Procedures. Solvents of 99.5% purity were used throughout this study. (COD)PdCl₂ was prepared according to literature procedures.³⁹ All other chemicals were obtained from common suppliers and used without further purification. ¹H and ¹³C spectra were recorded on a Bruker AC 300 P spectrometer. The spectra were referenced internally using the resonances of the solvent (¹H, ¹³C). Shifts are given in ppm; coupling constants, in

Table 5. Details of the Solid-State Structure Determination of 7, 8, 9, and 10

	7	8	9	10
formula	C ₉ H ₁₂ Cl ₂ N ₄ Pd, C ₂ H ₆ OS	C ₁₀ H ₁₄ Cl ₂ N ₄ Pd	C ₁₁ H ₁₆ Cl ₂ N ₄ Pd	C ₁₂ H ₁₈ Cl ₂ N ₄ Pd, C ₂ H ₆ OS
temp of measurement [K]	183(2)	198(2)	198(2)	198(2)
cryst syst, space group	triclinic, $P\bar{1}$	orthorhombic, $P2_12_12_1$	monoclinic, $P2_1$	triclinic, $P\bar{1}$
unit cell dimens:	7.7800(5), 8.2190(5), a, b, c [Å]	10.1400(15), 8.3940(4), 15.221(2)	8.1820(8), 15.3270(12), 11.9170(16)	8.7180(8), 9.0560(6), 12.9660(16)
α, β, γ [deg]	92.519(6), 102.089(6), 104.242(5)	90, 90, 90	90, 108.192(8), 90	75.813(7), 84.518(9), 78.738(6)
volume [Å ³], Z	826.17(9), 2	1295.5(3), 4	1419.8(3), 4	972.11(17), 2
cryst size [mm ³]	0.53 × 0.34 × 0.16	0.54 × 0.19 × 0.09	0.29 × 0.28 × 0.12	0.10 × 0.09 × 0.01
$F(000)$	432	728	760	480
θ range	3.43 to 26.40	3.42 to 26.40	3.61 to 28.00	3.81 to 26.40
no. of indep reflns	3388 [$R(\text{int}) = 0.0139$]	2640 [$R(\text{int}) = 0.0410$]	6837 [$R(\text{int}) = 0.0752$]	3988 [$R(\text{int}) = 0.0397$]
goodness-of-fit on F^2	1.004	1.042	1.080	1.059
final R indices	$R_1 = 0.0132$, [$I > 2\sigma(I)$]	$R_1 = 0.0188$, $wR_2 = 0.0374$	$R_1 = 0.0231$, $wR_2 = 0.0565$	$R_1 = 0.0250$, $wR_2 = 0.0600$
R indices (all data)	$R_1 = 0.0139$, $wR_2 = 0.0344$	$R_1 = 0.0233$, $wR_2 = 0.0384$	$R_1 = 0.0251$, $wR_2 = 0.0578$	$R_1 = 0.0295$, $wR_2 = 0.0625$
largest diff peak and hole [$e/\text{Å}^{-3}$]	+0.303 and -0.347	+0.288 and -0.300	+0.633 and -0.720	+0.859 and -0.952

Hz. Elemental analyses were performed by the microanalytical laboratory of our institute on a EuroVektor Euro EA-300 elemental analyzer.

5.2. Solid-State Structure Determination of 7, 8, 9, and 10.

Crystals for the solid-state structures of the palladium complexes **7**, **8**, and **10** could be obtained by slowly cooling a hot saturated solution of the complexes in DMSO. The crystals for the solid-state structure determination of **9** were obtained by condensing THF into a saturated DMSO solution of the complex. Preliminary examination and data collection were carried out on a NONIUS κ -CCD device with an Oxford Cryosystems cooling system at the window of a sealed fine-focus X-ray tube with graphite-monochromated Mo K_{α} radiation ($\lambda = 0.71073$ Å). The reflections were integrated. Raw data were corrected for Lorentz and polarization and, arising from the scaling procedure, for latent decay. An absorption correction was applied using SADABS. After merging, the independent reflections were all used to refine the structure. The structures were solved by a combination of direct methods and difference Fourier synthesis. All non-hydrogen atoms were refined with anisotropic displacement parameters. All hydrogen atoms were placed in calculated positions and refined using the riding model. Full-matrix least-squares refinements were carried out by minimizing $\sum w(F_o^2 - F_c^2)^2$. Details of the structure determinations are given in Table 5.^{40–43}

5.3. Synthesis of the Imidazolium Salts. 5.3.1. 1,1'-Dimethyl-3,3'-methylenebisimidazoliumdichloride (1). In a sealed tube 30 mmol of 1-methylimidazole (2.50 g) and 15 mmol of dichloromethane (1.27 g) are dissolved in 3 mL of PEG 200 and heated to 110 °C for 12 h. The white precipitate is filtered off and washed twice with 15 mL of THF. The product is obtained as a white hygroscopic powder.

Yield: 64.7% (2.42 g). ¹H NMR (DMSO-*d*₆, 25 °C): δ 9.86 (s, 2H, NCHN), 8.25 (s, 2H, NCH), 7.76 (s, 2H, NCH), 6.88 (s, 2H, NCH₂), 3.92 (s, 6H, NCH₃). ¹³C NMR (DMSO-*d*₆, 25 °C): δ 138.1 (NCHN), 124.0 (NCH), 121.9 (NCH), 57.3 (NCH₂N), 35.1 (NCH₃). Anal. Calcd for C₆H₁₄Cl₂N₄: C 43.38, H 5.66, N 22.49. Found: C 43.25, H 5.81, N 22.63.

5.3.2. 1,1'-Dimethyl-3,3'-(1,2-dimethylene)bisimidazolium-dichloride (2). In a sealed tube 24 mmol of 1-methylimidazole (2.00 g) and 12 mmol of 1,2-dichloroethane (1.19 g) are heated in

3 mL of PEG 200 for 12 h to 130 °C. A white hygroscopic solid is formed, filtered off, and washed twice with 15 mL of THF.

Yield: 78.2% (2.47 g). ¹H NMR (DMSO-*d*₆, 25 °C): δ 9.54 (s, 2H, NCHN), 7.86 (s, 2H, NCH), 7.77 (s, 2H, NCH), 4.82 (s, 4H, NCH₂), 3.86 (s, 6H, NCH₃). ¹³C NMR (DMSO-*d*₆, 25 °C): δ 137.4 (NCHN), 123.6 (NCH), 122.3 (NCH), 48.1 (NCH₂), 35.8 (NCH₃).

5.3.3. 1,1'-Dimethyl-3,3'-(1,3-trimethylene)bisimidazolium-dichloride (3). In a sealed tube 22 mmol of 1-methylimidazole (1.80 g) and 11 mmol of 1,3-dichloropropane (1.24 g) are heated for 48 h to 105 °C. A white hygroscopic solid is formed, filtered off, and washed twice with 15 mL of THF.

Yield: 76.5% (2.12 g). ¹H NMR (DMSO-*d*₆, 25 °C): δ 9.65 (s, 2H, NCHN), 7.96 (d, $J = 1.7$ Hz, 2H, NCH), 7.80 (d, $J = 1.5$ Hz, 2H, NCH), 4.30 (t, $J = 6.4$ Hz, 4H, NCH₂), 3.88 (s, 6H, NCH₃), 2.45 (qi, $J = 6.7$ Hz, 2H, CH₂CH₂CH₂). ¹³C NMR (DMSO-*d*₆, 25 °C): δ 137.1 (NCHN), 123.5 (NCH), 122.0 (NCH), 45.5 (NCH₂), 35.6 (NCH₃), 29.1 (CH₂CH₂CH₂).

5.3.1. 1,1'-Dimethyl-3,3'-(1,4-tetramethylene)bisimidazolium-dichloride (4). In a sealed tube 30 mmol of 1-methylimidazole (2.50 g) and 15 mmol of 1,4-dichlorobutane (1.91 g) are dissolved in 3 mL of PEG 200 and heated to 120 °C for 6 h. The white precipitate is filtered off and washed twice with 15 mL of THF.

Yield: 55.3% (2.42 g). ¹H NMR (DMSO-*d*₆, 25 °C): δ 9.62 (s, 2H, NCHN), 7.88 (s, 2H, NCH), 7.76 (s, 2H, NCH), 4.30 (t, $J = 6.2$ Hz, 4H, NCH₂), 3.87 (s, 6H, NCH₃), 1.78 (qi, $J = 6.2$ Hz, 4H, CH₂CH₂). ¹³C NMR (DMSO-*d*₆, 25 °C): δ 136.9 (NCHN), 123.6 (NCH), 122.3 (NCH), 47.7 (NCH₂), 35.7 (NCH₃), 25.9 (CH₂CH₂). Anal. Calcd for C₁₂H₂₀Cl₂N₄: C 49.50, H 6.92, N 19.24. Found: C 49.38, H 7.03, N 19.07.

5.4. Synthesis of Silver(I) Biscarbene Complexes. 5.4.1. Silver Complex 5. Bisimidazoliumsalt **3** (2.0 mmol, 0.554 g) and 1.9 mmol of Ag₂O (0.440 g) are dissolved in 120 mL of acetonitrile. The solution is stirred for 18 h at room temperature under exclusion of light, until a gray solid precipitates. The solution is filtered off, and the solid residue is dried in vacuo.

Yield: 93.3% (0.870 g). ¹H NMR (DMSO-*d*₆, 25 °C): δ 7.57 (s, 2H, NCH), 7.50 (s, 2H, NCH), 3.88 (bt, $J = 5.9$ Hz, 4H, NCH₂), 3.71 (s, 6H, NCH₃), 2.40 (bs, 2H, CH₂CH₂CH₂). ¹³C NMR (DMSO-*d*₆, 25 °C): δ 179.1 (NCN), 124.1 (NCH), 120.6 (NCH), 46.5 (NCH₂), 38.1 (NCH₃), 29.4 (CH₂CH₂CH₂). Anal. Calcd for C₁₁H₁₆-Ag₂Cl₂N₄: C 26.91, H 3.29, N 11.41. Found: C 26.91, H 3.13, N 11.20.

5.4.2. Silver Complex 6. Bisimidazoliumsalt **4** (1.0 mmol, 0.267 g) and 0.95 mmol of Ag₂O (0.220 g) are dissolved in 50 mL of acetonitrile. The solution is stirred for 18 h at room temperature under exclusion of light, until a white solid precipitates. The solution

(40) SADABS, Area Detector Absorption and Other Corrections, 2.03; Bruker: Delft, Netherlands, 2002.

(41) Spek, A. L. *J. Appl. Crystallogr.* **2003**, *36*, 7–13.

(42) Altomare, A.; Cascarano, G.; Giacovazzo, C.; Guagliardi, A.; Burla, M. C.; Polidori, G.; Camalli, M. *J. Appl. Cryst.* **1994**, *27*, 435–436.

(43) Sheldrick, G. M. *SHELXL-97*, Program for the Refinement of Structures; Universität Göttingen, 1997.

is filtered off, and the solid residue is washed with 10 mL of acetonitrile and dried in vacuo.

Yield: 92.5% (0.444 g). ^1H NMR (DMSO- d_6 , 25 °C): δ 7.47 (s, 2H, NCH), 7.42 (s, 2H, NCH), 4.12 (bs, 4H, NCH₂), 3.78 (s, 6H, NCH₃), 1.79 (bs, 4H, CH₂CH₂). ^{13}C NMR (DMSO- d_6 , 25 °C): δ 179.4 (NCN), 123.0 (NCH), 121.8 (NCH), 41.1 (NCH₂), 35.8 (NCH₃), 27.9 (CH₂CH₂). Anal. Calcd for C₁₂H₁₈Ag₂Cl₂N₄: C 28.54, H 3.59, N 11.09. Found: C 28.72, H 3.82, N 11.15.

5.5. Syntheses of the Palladium Complexes. 5.5.1. 1,1'-Dimethyl-3,3'-methylene-diimidazole-2,2'-diylidene-palladium(II)dichloride (7). Pd(OAc)₂ (1.34 mmol, 0.300 g) and 1.34 mmol of **1** (0.333 g) are dissolved in 10 mL of DMSO and heated for 2 h to 60 °C, 2 h to 80 °C, and 2 h to 100 °C. During the reaction the solution turns from dark red to yellow. Then the solvent is removed in vacuo, and the resulting residue is washed twice with 3 mL of methanol. The product is obtained as a white powder in 70.7% yield.

Yield: 70.7% (0.335 g). Melting point: >320 °C. ^1H NMR (DMSO- d_6 , 25 °C): δ 7.58 (s, 2H, NCH), 7.31 (s, 2H, NCH), 6.25 (s, 2H, NCH₂N), 3.95 (s, 6H, NCH₃). ^{13}C NMR (DMSO- d_6 , 25 °C): δ 156.7 (NCN), 123.0 (NCH), 121.1 (NCH), 62.1 (NCH₂N), 37.7 (NCH₃). Anal. Calcd for C₉H₁₂Cl₂N₄Pd: C 30.58, H 3.42, N 15.85. Found: C 30.59, H 3.38, N 15.70.

5.5.2. 1,1'-Dimethyl-3,3'-(1,2-dimethylene)diimidazole-2,2'-diylidene-palladium(II)dichloride (8). Bisimidazoliumsalt **2** (0.76 mmol, 0.200 g) and 0.76 mmol of Pd(OAc)₂ (0.171 g) are dissolved in 5 mL of DMSO and heated for 0.5 h first to 60 °C while a clear deep red solution is formed. The mixture is then cooled to 40 °C and stirred for at least 4 h at this temperature until a white powder starts to precipitate. Then the reaction mixture is again heated for 3 h to 60 °C, 3 h to 80 °C, 2 h to 100 °C, and 2 h to 130 °C. After the reaction the solvent is removed in vacuo and the white residue is washed with 2 mL of water and 2 mL of THF.

Yield: 69.4% (0.194 g). Melting point: 304 °C (dec). ^1H NMR (DMSO- d_6 , 25 °C): δ 7.37 (s, 2H, NCH), 7.34 (s, 2H, NCH), 5.18 (bs, 2H, -CH₂-CH₂-), 4.47 (bd, J = 6.8 Hz, 2H, -CH₂-CH₂-), 3.88 (s, 6H, NCH₃). ^{13}C NMR (DMSO- d_6 , 25 °C): δ 123.7 (NCH), 122.5 (NCH), 46.9 (NCH₂), 37.9 (NCH₃) [C_{carbene} not detected]. Anal. Calcd for C₁₀H₁₄Cl₂N₄Pd: C 32.68; H 3.84; N 15.24. Found: C 32.78; H 3.95; N 14.85.

5.5.3. 1,1'-Dimethyl-3,3'-(1,3-trimethylene)diimidazole-2,2'-diylidene-palladium(II)dichloride (9). In 15 mL of DMSO 1.0 mmol of **5** (0.491 g) and 1 mmol of 1,5-cyclooctadiene-palladium(II) dichloride (0.285 g) are stirred under exclusion of light for 12 h. The precipitated Ag(I)Cl is filtered off, and the solvent of the resulting solution is removed in vacuo until a white residue appears. This residue is washed with 3 mL of acetonitrile, and then the product is extracted with 2 × 15 mL of water. The water is removed in vacuo, and the solid residue is washed with 10 mL of THF and dried.

Yield: 92.0% (0.351 g). Melting point: 288 °C (dec). ^1H NMR (DMSO- d_6 , 25 °C): δ 7.32 (s, 2H, NCH), 7.29 (s, 2H, NCH), 4.84 (t, J = 11.8 Hz, 2H, NCH₂), 4.35 (m, 2H, NCH₂), 3.94 (s, 6H, NCH₃), 2.34–2.29 (m, 1H, CH₂CH₂CH₂), 1.73–1.71 (m, 1H, CH₂CH₂CH₂). ^{13}C NMR (DMSO- d_6 , 25 °C): δ 123.0 (2 × NCH), 51.4 (NCH₂), 37.5 (NCH₃), 31.3 (CH₂CH₂CH₂) [C_{carbene} not detected]. Anal. Calcd for C₁₁H₁₆Cl₂N₄Pd: C 34.62, H 4.23, N 14.68. Found: C 34.74, H 4.33, N 14.67.

5.5.3. 1,1'-Dimethyl-3,3'-(1,4-tetramethylene)diimidazole-2,2'-diylidene-palladium(II)dichloride (10). In 8 mL of DMSO 0.5 mmol of **6** (0.253 g) and 0.5 mmol of 1,5-cyclooctadiene-palladium(II) dichloride (0.143 g) are stirred under exclusion of light for 24 h. The precipitated Ag(I)Cl is removed by centrifugation, then the solvent of the resulting solution is removed in vacuo until a white residue appears. The product is extracted from this residue with 2 × 10 mL of water. The water is removed in vacuo, and the solid residue is washed again with 10 mL of THF and dried.

Yield: 24.3% (0.048 g). Melting point: 206 °C (dec). ^1H NMR (DMSO- d_6 , 25 °C): δ 7.32 (s, 2H, NCH), 7.30 (s, 2H, NCH), 5.05 (m, 2H, NCH₂), 4.18 (m, 2H, NCH₂), 3.98 (s, 6H, NCH₃), 2.10–1.93 (m, 2H, CH₂CH₂CH₂CH₂), 1.09–0.92 (m, 2H, CH₂CH₂CH₂CH₂). ^{13}C NMR (DMSO- d_6 , 25 °C): δ 158.5 (NCN), 123.6 (NCH), 121.2 (NCH), 45.3 (NCH₂), 42.0 (NCH₂), 40.2 (CH₂CH₂CH₂), 37.0 (NCH₃), 25.1 (CH₂CH₂CH₂). Anal. Calcd for C₁₂H₁₈Cl₂N₄Pd·0.5DMSO: C 35.92, H 4.87, N 12.89, S 3.69. Found: C 35.84, H 4.83, N 12.45, S 3.42.

5.6. Catalytic CH Activation of Methane. All reactions were conducted in a 160 mL Hastelloy C-2000 autoclave (Parr) in the presence of a palladium catalyst (0.168 mmol) and K₂S₂O₈ (16.8 mmol) in a mixture of trifluoroacetic acid and its anhydride (32 mL/24 mL). The reaction vessel is pressurized with 30 bar of methane and heated to 90 °C. A gas injection stirrer is started with 500 rpm when the final temperature is reached. After a reaction time of 17 h, stirring and heating are stopped and the reaction mixture is cooled to room temperature. The autoclave is depressurized and the reaction mixture is analyzed by gas chromatography with an Agilent 6850 Series II Networked GC, equipped with an FID detector and a Macherey-Nagel Optima-210-0.25 μm column (30 m × 0.25 mm). Quantification of the trifluoroacetic acid methyl ester is done by adding 25 μL of *p*-xylene to 1.00 mL of the reaction mixture after the reaction as an external standard and injection of this mixture into the GC. All GC measurements are repeated four times; given values are averaged over all measurements. The turnover number (TON) is defined as (mol product)/(mol Pd).

5.7. Catalytic Heck Reaction. All reactions were carried out under a dry nitrogen atmosphere. *N,N*-Dimethylacetamide was distilled prior to use and stored over 4 Å molecular sieves under nitrogen. GC-MS spectra were measured on a Hewlett-Packard GC G1800A system. The conversion was measured using diethylene glycol di-*n*-butyl ether as internal standard. The turnover number (TON) is defined as (mol product)/(mol Pd), while the turnover frequency (TOF) is defined as (mol product)/[(mol Pd)(reaction time in h)].

General Procedure for the Mizoroki–Heck Reaction. A 10 mL Schlenk flask equipped with a reflux condenser was degassed and put under an atmosphere of nitrogen. It is charged with aryl halides (1 mmol), styrene (1.4 mmol), anhydrous sodium acetate (1.1 mmol), diethylene glycol di-*n*-butyl ether, the denoted amount of catalyst (mol % catalyst is given relative to amount of styrene), and 5 mL of *N,N*-dimethylacetamide. After that the flask is placed in a preheated oil bath at 140 °C. Aliquots (0.2 mL) were removed from the reaction mixture after a fixed time period and added to dichloromethane (10 mL) to observe the reaction progress. The organic portion is washed four times with 5 mL of water and dried with anhydrous MgSO₄. The solution is filtered, diluted with 5 mL of dichloromethane, and analyzed by gas chromatography.

5.8. Computational Details. All calculations were performed with Gaussian03.⁴⁴ The density functional hybrid model

(44) Frisch, M. J.; G. W. T.; Schlegel, H. B.; Scuseria, G. E.; Robb, M. A.; Cheeseman, J. R.; Montgomery, J. A., Jr.; Vreven, T.; Kudin, K. N.; Burant, J. C.; Millam, J. M.; Iyengar, S. S.; Tomasi, J.; Barone, V.; Mennucci, B.; Cossi, M.; Scalmani, G.; Rega, N.; Petersson, G. A.; Nakatsuji, H.; Hada, M.; Ehara, M.; Toyota, K.; Fukuda, R.; Hasegawa, J.; Ishida, M.; Nakajima, T.; Honda, Y.; Kitao, O.; Nakai, H.; Klene, M.; Li, X.; Knox, J. E.; Hratchian, H. P.; Cross, J. B.; Bakken, V.; Adamo, C.; Jaramillo, J.; Gomperts, R.; Stratmann, R. E.; Yazyev, O.; Austin, A. J.; Cammi, R.; Pomelli, C.; Ochterski, J. W.; Ayala, P. Y.; Morokuma, K.; Voth, G. A.; Salvador, P.; Dannenberg, J. J.; Zakrzewski, V. G.; Dapprich, S.; Daniels, A. D.; Strain, M. C.; Farkas, O.; Malick, D. K.; Rabuck, A. D.; Raghavachari, K.; Foresman, J. B.; Ortiz, J. V.; Cui, Q.; Li, A. G.; Clifford, S.; Cioslowski, J.; Stefanov, B. B.; Liu, G.; Liashenko, A.; Piskorz, P.; Komaromi, I.; Martin, R. L.; Fox, D. J.; Keith, T.; Al-Laham, M. A.; Peng, C. Y.; Nanayakkara, A.; Challacombe, M.; Gill, P. M. W.; Johnson, B.; Chen, W.; Wong, M. W.; Gonzalez, C.; Pople, J. A. *Gaussian 03*, Revision C.02; Gaussian, Inc.: Wallingford, CT, 2004.

Becke3LYP^{45–48} was used together with the valence double- ζ basis set 6-31G(d). For palladium the Hay–Wadt ECP basis set⁴⁹ was used. No symmetry or internal coordinate constraints were applied during optimizations. All reported intermediates were verified as true minima by the absence of negative eigenvalues in the vibrational frequency analysis. Approximate free energies were obtained through thermochemical analysis of the frequency calculation, using the thermal correction to the Gibbs free energy as reported by Gaussian03. This takes into account zero-point effects, thermal enthalpy corrections, and entropy. All energies reported in

(45) Lee, C.; Yang, W.; Parr, R. G. *Phys. Rev. B: Condens. Matter* **1988**, *37* (2), 785–789.

(46) Vosko, S. H.; Wilk, L.; Nusair, M. *Can. J. Phys.* **1980**, *58* (8), 1200–1211.

(47) Stephens, P. J.; Devlin, F. J.; Chabalowski, C. F.; Frisch, M. J. *J. Phys. Chem.* **1994**, *98* (45), 11623–11627.

(48) Becke, A. D. *J. Chem. Phys.* **1993**, *98* (7), 5648–5652.

(49) Hay, P. J.; Wadt, W. R. *J. Chem. Phys.* **1985**, *82*, 299.

this paper, unless otherwise noted, are energies at 298 K and 1 atm. Frequencies remain unscaled.

Acknowledgment. We are grateful to the “Deutsche Forschungsgemeinschaft” (DFG) and the “Fonds der Chemischen Industrie” (FCI) for financial support. S.A. thanks the “Konrad-Adenauer-Stiftung” (KAS) for their support.

Supporting Information Available: Crystallographic data for **7**, **8**, **9**, and **10**. This material is available free of charge via the Internet at <http://pubs.acs.org>. CCDC-619038 (**7**), -619039 (**8**), -619036 (**9**), and -619037 (**10**) contain the supplementary crystallographic data for this paper. These data can be obtained free of charge from the Cambridge Crystallographic Data Centre via www.ccdc.cam.ac.uk/data_request/cif.

OM060577A